# INVERSION OF STOKES VECTOR PROFILES IN TERMS OF A 3-COMPONENT MODEL

P.N. BERNASCONI and S.K. SOLANKI
*Institute of Astronomy, ETH Zentrum, CH-8092 Zurich, Switzerland*

**Abstract.** Various spectropolarimetric observations show peculiar Stokes profiles that reveal the coexistence of at least two magnetic components in the same resolution element. An example is given by observations of the full Stokes vector in a complex active region performed with the ZIMPOL I Stokes polarimeter. In order to deduce the physical parameters of the observed regions from such measured profiles, we have extended an existing inversion code, so that it can now fit the data with models composed of up to three different atmospheric components. Two of these components are magnetic and may possess different field strengths, field geometries, temperature stratifications, and velocity fields. The third component describes the field free atmosphere surrounding the magnetic features.

The so extended inversion code has then been applied to the ZIMPOL I data. In this paper we present and discuss sample fits. The code is able to reproduce the observed complex Stokes profiles with good accuracy and provides physical parameters for both of the coexisting magnetic atmospheres. Inversion tests with a 2-component model (with one magnetic and one non-magnetic component) applied to the same profiles do not reproduce the measurements sufficiently well.

**Key words:** Sun – Polarization – Magnetic fields – Diagnostic techniques

## 1. Introduction

With the instrumentation currently available it is generally impossible to fully resolve small solar magnetic features. Consequently both magnetic and non-magnetic atmospheric components are often present in the same resolution element. Using polarimetric techniques it is possible to overcome this problem, since only the magnetic component produces polarized line profiles, Stokes $Q$, $U$, and $V$. The non-magnetic component contributes only to the intensity, Stokes $I$.

The interpretation of observed Stokes profiles is much more complex if more than one magnetic component is present in the same resolution element. The polarized profiles, in particular Stokes $V$, do not look "simple" any more and it is not so straightforward to determine the atmospheric parameters, such as magnetic field strength $B$, field geometry (angles $\gamma$ and $\chi$), and temperature stratification $T(\tau)$, for each component. Although complex Stokes profiles have been successfully interpreted in the past, they always had to be fit manually (i.e., without an inversion approach). Stenflo (1968) first introduced the concept of multicomponent models. Skumanich and Lites (1991) observed complex Stokes $V$ profiles in the line Fe I 6302.5 Å

*Solar Physics* **164**: 277–290, 1996.

recorded at the neutral line between two sunspots with different polarities. They interpreted the measured profiles by manually fitting them with a model possessing two magnetic components. Martínez Pillet *et al.* (1994) found strongly distorted Stokes $V$ profiles that they interpreted as the superposition of Stokes $V$ spectra belonging to two different magnetic components with opposite polarities. One of the two components was highly red-shifted with respect to the other. Rüedi *et al.* (1992a,b) manually analyzed numerous Stokes $V$ profiles of 1.56 $\mu$m lines exhibiting clear signatures of two magnetic components. In this case the analysis is simplified by the larger Zeeman splitting of infrared magnetic lines.

Inversion techniques have so far not been applied to the analysis of complex Stokes profiles and Stokes inversion codes (e.g., Skumanich and Lites, 1987; Ruiz Cobo and Del Toro Iniesta, 1992; Solanki *et al.*, 1992a,b) have previously been incapable of inverting such profiles. Here we present an inversion code capable of reproducing complex Stokes profiles. As an illustration we apply it to anomalous Stokes profiles of spectral lines in the visible, which need a model with two magnetic and one non-magnetic component to be correctly reproduced. The main aim of this work is to demonstrate the feasibility of applying an automated fit procedure with a 3-component model to complex Stokes profiles in the visible.

## 2. Observational data

The present paper is based on observations performed at the Swedish Vacuum Solar Telescope on La Palma (Canary Islands) on May 13, 1993 with the Zürich Imaging Stokes Polarimeter (ZIMPOL I) together with U. Egger, C.U. Keller, H.P. Povel and P. Steiner (see Stenflo, 1991; Povel *et al.*, 1990, 1994, and Povel, 1995 for an overview of the polarimeter). We recorded the complete Stokes vector of the three well known lines Fe I 5247.1 Å ($g_{\rm eff} = 2.0$), Fe I 5250.2 Å ($g = 3.0$) and Fe I 5250.7 Å ($g_{\rm eff} = 1.5$) in an active region belonging to NOAA group No. 7500 located at 18°N, 33°W. The angle between the normal to the solar surface and the line of sight was $\theta = 40°$, which corresponds to $\mu = \cos\theta = 0.76$.

At the time of the observations the instrument was working with a single CCD camera placed in the focus of the spectrograph, so that it was only possible to record Stokes $I$ plus one other Stokes parameter ($Q$, $U$ or $V$) in a single exposure. We obtained the full Stokes vector sequentially by measuring each polarized Stokes parameter in turn, with an integration time of 1 s per measurement and an interval of $\sim$ 150 ms between two consecutive measurements. The sequence of three exposures was repeated seven times, after which the seven images for each Stokes parameter were co-added, so that the net integration time for each parameter was 7 s. This procedure

ensures quasi-simultaneity, even if strictly simultaneous images of all four Stokes parameters presently cannot be obtained with a single CCD (but should become possible with the next generation of polarimeters, e.g., ZIMPOL II, see Keller *et al.*, 1995). For one slit position the total integration time per Stokes image was 21 s, and the noise level was approximately 0.25% rms in units of the continuum intensity. Each set of four reduced images contains 120 spectra each in Stokes $I$, $Q$, $U$ and $V$, ranging from 5246.3 Å to 5251.5 Å, with a spectral resolving power of 175 000 and a pixel size in the spatial direction of $0.4''$. More information on the observations and analysis is given by Bernasconi *et al.* (in preparation).

The presence of three oblique reflections in the optical train of the Swedish Vacuum Solar Telescope introduces a large amount of instrumental polarization and cross-talk into the Stokes measurements. To free the data from this unwanted effect, we developed a theoretical model for the instrumental polarization of the telescope. The complex refractive indices of the three mirrors were considered as free parameters. They were determined by fitting the theoretical curves describing the daily behavior of the instrumentally produced continuum polarization to the observed values recorded at different times of the day. With this procedure we were able to directly fit only the first column of the telescope Mueller matrix, i.e. we could correctly determine only three elements of the matrix. The remaining elements were, however, consistently calculated by means of the theoretical Mueller matrix for reflections by mirrors given by Stenflo (1994) using the refractive indices derived from the observations. The so deduced telescope Mueller matrix, transformed to the time at which the solar Stokes spectrum we analyze was recorded, was applied to the Stokes measurements. The resulting Stokes images are free from the effects of instrumental polarization with an accuracy better than 0.5%, which corresponds to twice the rms noise level.

The remainder of the data reduction follows procedures standard for ZIMPOL. The noise level was additionally reduced by a factor of 1.5 using a Fourier low-pass filter in the spectral direction.

Although most of the Stokes profiles along the slit are "normal", in shape a number of them are "complex", i.e. they show signs of two magnetic components. The solid lines in Figs. 1, 2 and 3 show three examples of reduced Stokes profiles requiring two magnetic components to be fit. In Figs. 1 and 2 the presence of a second component is clearly visible in the profile shape of Stokes $V$ (it is distorted relative to the usual almost antisymmetric profile shape well beyond the possible influence of remaining uncompensated cross-talk). The influence of a possible second magnetic component is more subtle on the profiles plotted in Fig. 3: it mainly exhibits itself through the wavelength shift of $V$ relative to $Q$ and $U$.

## 3. Inversions

To derive the magnetic field strength, field orientation, and temperature stratification we used an inversion code that fits observed Stokes profiles using a non-linear least-squares technique (Levenberg-Marquardt, see Press *et al.*, 1990) with synthetic profiles that are solutions of the radiative transfer equations for polarized light. The inversion code is basically the same as that used by Bernasconi *et al.* (1995) and described and applied by Solanki *et al.* (1992a,b) and Emonet (1992). It has, however, been modified to allow complex Stokes profiles such as those plotted in Figs. 1–3 to be fit. The main features of the modifications are discussed below.

### 3.1. 3-COMPONENT ATMOSPHERIC MODEL

To allow the inversion code to fit complex Stokes profiles of the type illustrated in Figs. 1, 2, and 3, we modified the code by introducing the possibility of inverting Stokes profiles based on a 3-component model. The first two components are magnetic. They may possess different field strength, magnetic field geometries, temperature stratifications and velocity fields. The third component is field free and usually describes the quiet sun.

Two filling factors $\alpha_1$ and $\alpha_2$ describe the fraction of the spatial resolution element covered by the first and the second magnetic components, respectively. The remaining portion of the resolution element, i.e. $1 - \alpha_1 - \alpha_2$, is covered by the third, field-free component. $\alpha_1$ and $\alpha_2$ are free parameters that have to be determined during the fit procedure. First the Stokes vector resulting from each component is calculated, then a linear combination of the three Stokes vectors weighted by their respective filling factors is determined:

$$\begin{aligned} I_{\rm res} &= I_1\,\alpha_1 + I_2\,\alpha_2 + I_3\,(1-\alpha_1-\alpha_2)\,, \\ Q_{\rm res} &= Q_1\,\alpha_1 + Q_2\,\alpha_2\,, \\ U_{\rm res} &= U_1\,\alpha_1 + U_2\,\alpha_2\,, \\ V_{\rm res} &= V_1\,\alpha_1 + V_2\,\alpha_2\,, \end{aligned} \tag{1}$$

where the indices refer to the contributions of the components 1, 2, and 3, respectively, and $(I_{\rm res}\,,\,Q_{\rm res}\,,\,U_{\rm res}\,,\,V_{\rm res})^{\rm T}$ is the transpose of the resulting Stokes vector which is compared to the observations.

### 3.2. FREE PARAMETERS AND MODEL ATMOSPHERES

Each component is described by a model atmosphere. Key parameters describing each atmosphere are allowed to vary and be determined by the fitting procedure. The remainder of the parameters are calculated self-consistently therefrom. We distinguish between two types of free parameters,

those which depend on the spectral lines and those which do not. We first discuss the latter.

The spectral line-independent free parameters in the magnetic model atmospheres are the temperature $T$, the field strength $B$, the filling factor $\alpha$, the inclination $\gamma$ of the field lines with respect to the line of sight, and the field azimuth $\chi$ counted counterclockwise starting from the geocentric W direction. With the exception of the temperature, all these parameters are depth independent. In some cases the field strength is also allowed to vary with depth, i.e. a field gradient $\nabla B = \partial B/\partial \log \tau$ is introduced as a further free parameter when it reproduces the real magnetic field structure in the solar atmosphere better. A magnetic gradient was used only when the measured Stokes profiles appeared "simple", i.e. a single magnetic component was sufficient to reproduce the observed spectra. In the cases where two magnetic atmospheres were needed we preferred to have a simple model for the magnetic structure of each component, in order to keep the number of free parameters as small as possible. Note that the inversion code allows $B(\tau)$ to be determined consistently from horizontal pressure balance if $B$ is specified at a single height, but we have chosen not to use this option (which corresponds to the thin-tube approximation), since many of the inverted spectra lie in penumbra-like structures or are affected by pore magnetic fields, to which the thin-tube approximation does not apply.

Although the temperature $T$ is a function of the continuum optical depth $\tau$ (or height $z$) we prefer to determine it only at a single $\tau$ value in the case of magnetic atmospheres. $T(\log \tau_{5000} = -1.5)$ is allowed to vary, while $T$ at other $\tau$ values is determined by linearly interpolating between the two nearest temperature stratifications of the empirical plage flux tube model of Solanki and Brigljevíc (1992), the quiet-sun atmosphere of Maltby *et al.* (1986), and the umbral model M of Maltby *et al.* (1986).

For the quiet-sun component the entire temperature stratification of the Maltby *et al.* (1986) quiet-sun model atmosphere is simply translated until it passes through the prescribed temperature at $\log \tau_{5000} = -1.5$.

The parameters calculated consistently from $T(\tau)$ are the geometrical depth $z(\tau)$, the electron pressure $P_{\rm el}(\tau)$, the gas pressure $P_{\rm gas}(\tau)$, and the gas density $\rho_{\rm gas}(\tau)$.

For the Doppler width of the microturbulent velocity distribution $\xi_{\rm mic}$ we chose a constant value of 1.0 km/s for all the atmospheric components.

In addition, for each magnetic component we assigned a different Doppler shift $\Delta\lambda_l$ and macroturbulence $\xi_{{\rm mac},l}$ to each spectral line (the index $l$ labels the three observed spectral lines: $l$ = 5247.1 Å, 5250.2 Å, 5250.7 Å). These parameters were kept free. In this way we could take into account also the effect of different velocities in the various atmospheric components. To reduce the number of free parameters in our model, we decided to force $\xi_{\rm mac}$

for the two lines Fe I 5247.1 Åand 5250.2 Å to be the same, since they have almost the same atomic parameters (Solanki, 1987).

### 3.3. Tests

In order to test the extension of the inversion code to three components we fit a number of infrared Stokes $I$ and $V$ spectra of $\lambda$ 15648 Å and $\lambda$ 15652 Å that obviously required two magnetic components. These data had earlier been analyzed by Rüedi *et al.* (1992). Our results, based on the automated inversion procedure, were in good agreement with their findings which are based on manual fits. The large Zeeman splitting of the infrared lines made the fitting procedure easier and faster.

Once the inversion code had passed these tests, we applied it to the observed Stokes $V$, $Q$, and $U$ spectra of the visible lines that are discussed in Section 2.

## 4. Examples of inversions with a 3-component model

We now present and discuss three examples of fits to complex Stokes spectra. We aim to show that for these profiles a model with two magnetic components in addition to the quiet-sun component reproduces the data much better than a model with a single magnetic component, at least as long as extremely strong velocity-magnetic gradient combinations along the line-of-sight (LOS) are not allowed.

We decided not to fit the Stokes $I$ profiles because they are heavily influenced by the non-magnetic atmosphere surrounding the magnetic features and are not required to determine the strength and orientation of the magnetic field on which our major interest was focused. Consequently, in the following figures we do not plot the synthetic Stokes $I$ profiles.

Table I lists the most important atmospheric parameters referring to the best fit curves shown in the following Figures. $\gamma$ is the field inclination with respect to the LOS (angles larger than 90° signify field lines oriented away from the observer), $\chi$ the field azimuth counted counterclockwise from the heliocentric W direction, and $T$ the temperature at continuum optical depth $\log \tau_{5000} = -1.5$. In the last column the relative flow velocities $\Delta\lambda$ between the two magnetic components along the LOS are listed. They have been derived by computing the difference of the Doppler shifts for the two components (since the spectrograph was not absolutely calibrated, only relative Doppler shifts are meaningful). $\Delta\lambda = 1$ km/s means that the velocity flow in the first magnetic component is 1 km/s faster towards the observer than the flow in the second component. To determine the errors in the best-fit parameters we repeated the fits several times with different initial parameters and compared the various resulting fits with each other. This procedure

TABLE I
Parameters derived from the inversion.

| Fig. No. | Comp. No. | $B$ [G] | $\alpha$ | $\gamma$ | $\chi$ | $T$ [K] | $\Delta\lambda$ [km/s] |
|---|---|---|---|---|---|---|---|
| 1 | 1 | 1450 | 0.30 | 133 | 33 | 4680 | 1.0 |
| | 2 | 1830 | 0.24 | 31 | 70 | 4430 | |
| 2 | 1 | 781 | 0.64 | 118 | 24 | 5340 | 3.3 |
| | 2 | 2187 | 0.23 | 54 | 42 | 4640 | |
| 3 | 1 | 1300 | 0.38 | 117 | 44 | 4460 | 1.1 |
| | 2 | 1580 | 0.41 | 43 | 87 | 4370 | |
| 4 | | 1290 | 0.36 | 60 | 49 | 4380 | — |

allowed us to test the uniqueness of the results, which turned out to be quite good, especially for the simpler profiles. We estimated an accuracy of 100 G for the field strength, 0.05 for the filling factors, 5° for $\gamma$ and $\chi$, 100 K for the temperature, and 0.2 km/s for $\Delta\lambda$.

The first example we wish to discuss is shown in Figure 1. The observed profiles refer to a slit position between two regions with reversed magnetic polarity (relative to the LOS). The Stokes $V$ profiles look unusual, having a profile shape more typical of $Q$ or $U$. This is however common for $V$ spectra along apparent neutral lines (see for example Skumanich and Lites, 1991; Sánchez Almeida and Lites, 1992; Rüedi *et al.*, 1992b). Since the observed region lies outside sunspots (at the edge of a pore without a visible penumbra) it is likely that two magnetic components with similar field strengths but with opposite magnetic polarities and different flow velocities coexist in the same resolution element (within penumbrae $V$ profiles of the same general shape can be produced by a single magnetic component: Sánchez Almeida and Lites, 1992; Solanki *et al.*, 1994). The discontinuity in the synthetic profiles around $\lambda = 5250.5$ Å is due to an overlap of the selected spectral wavelength ranges over which these two lines are synthesized. Note how well the $V$ and $Q$ profiles are reproduced. The fit of Stokes $U$ is of lower quality, possibly due to the presence of a third, weak magnetic component almost perpendicular to the LOS, which was not taken into account in our model (the wavelength shift between $U$ and $V$ supports this interpretation, see discussion of Fig. 3 below). Another possibility is the presence of significant gradients of magnetic and velocity fields in one or both of the components (this is supported by the asymmetry of the Stokes $U$ profiles).

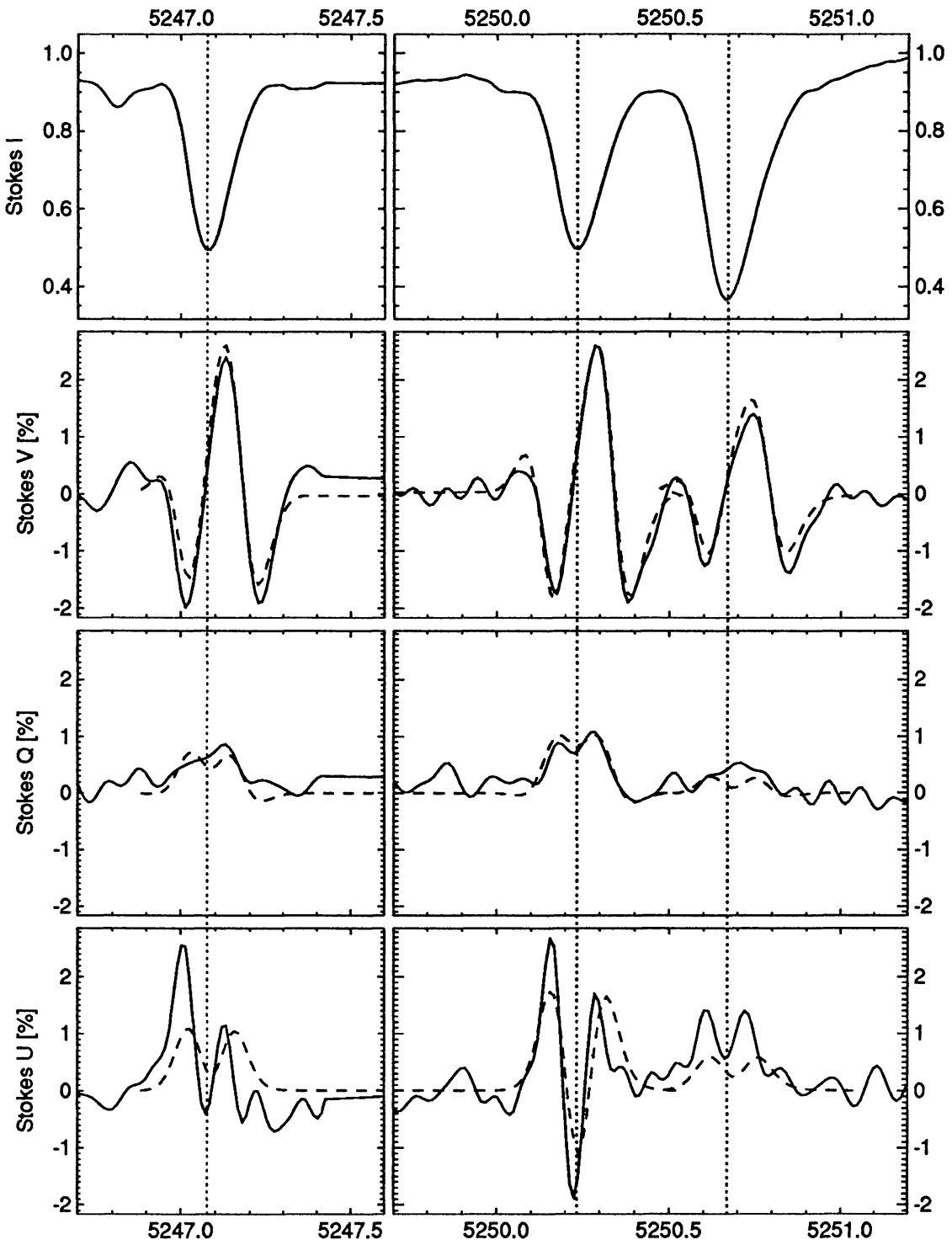


Fig. 1. Observed (solid) and synthetic (dashed) Stokes profiles. A model with two magnetic components of opposite polarity, $B_1 = 1450$G, $\gamma_1 = 133°$, and $B_2 = 1830$G, $\gamma_2 = 31°$, and a Doppler shift between the two components of 1.0 km/s was used to fit the data. The vertical dotted lines mark the wavelengths of the Stokes $I$ minima.

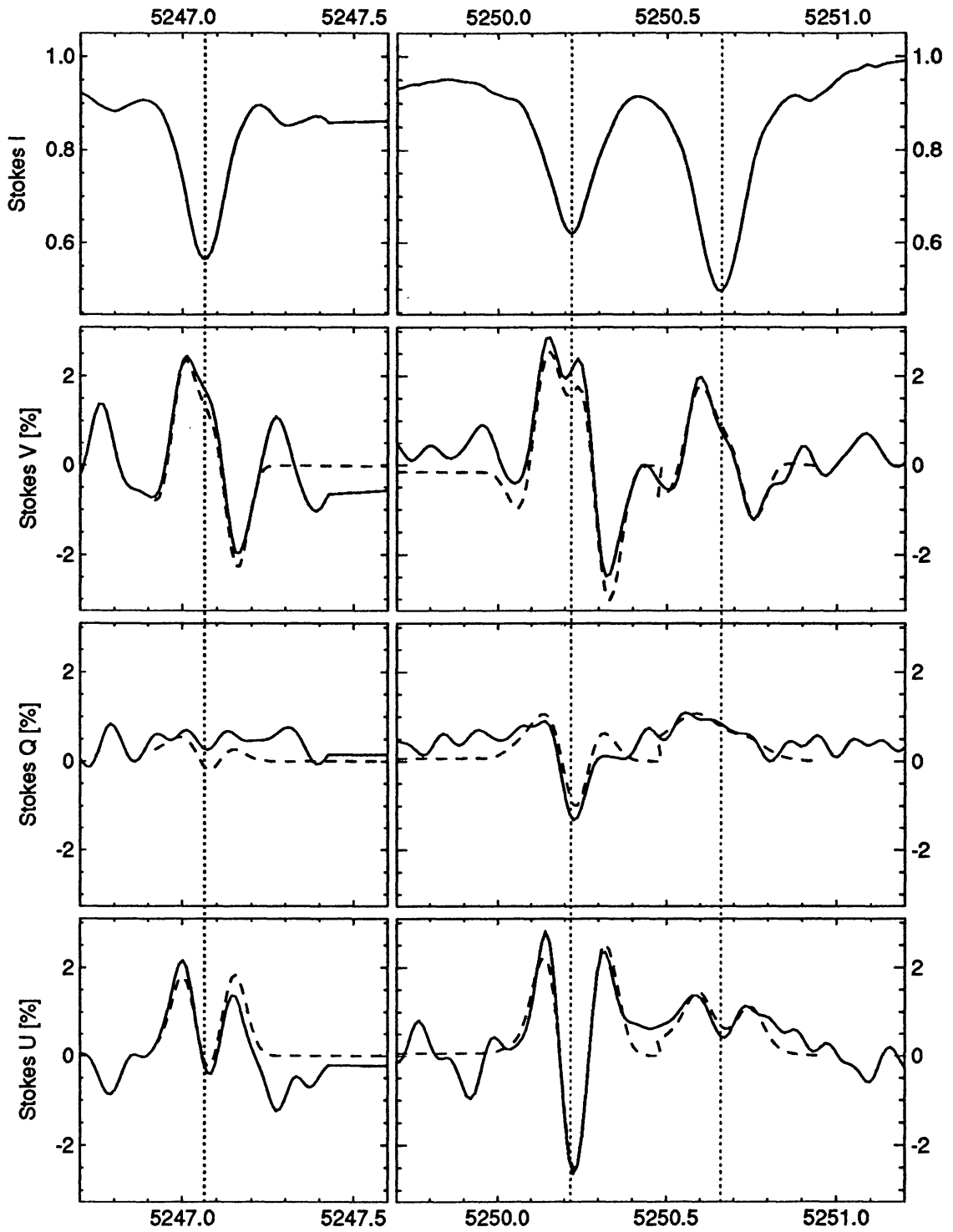


Fig. 2. Observed (solid) and synthetic (dashed) Stokes profiles. A model with two magnetic components of opposite polarity, $B_1 = 780$ G, $\gamma_1 = 118°$, and $B_2 = 2190$G, $\gamma_2 = 54°$, and a Doppler shift between the two components of 3.3 km/s was used to fit the data. The vertical dotted lines mark the wavelengths of the Stokes $I$ minima.

As a second example we plot in Fig. 2 another set of complex Stokes profiles. The blue wing of Stokes $V$ is much broadener than the red wing, and the Fe I 5250.2 Å Stokes $V$ profiles exhibit a double peak that is not due to noise. It is suggestive of the presence of (at least) two magnetic components. Once more the 3-component model inversion finds synthetic profiles that are in good agreement with the observations. These data were recorded very close to a pore, which contributes to the strong component deduced from the fit (Component No. 2 in Tab. I), while the weaker component (Component No. 1) probably corresponds to the canopy of another pore located in the vicinity. This interpretation also explains the large temperature difference between the two components.

The evidence for two magnetic components is less obvious in Fig. 3. In this case the Stokes $V$ profiles look almost "normal", but for all the lines we notice a strong wavelength shift between the zero crossing of $V$, the minimum of Stokes $I$, and the core of the $\pi$ components for Stokes $Q$ and $U$. We can explain these shifts by considering two magnetic components with slightly different velocity fields, having different inclinations relative to the LOS. The component more aligned with the LOS (Component No. 1) contributes to the Stokes $V$ profiles much more than the more transverse one (Component No. 2). The latter, however, dominates the Stokes $Q$ and $U$ signals. Finally, the difference between the velocity fields in the two atmospheres gives rise to the observed shifts between the various Stokes profiles.

Our inversion code with the 3-component model easily separated the two magnetic components, and provided synthetic Stokes profiles that match the observations relatively satisfactorily. For comparison purposes we inverted the same set of profiles by applying a model with just a single magnetic component. The result is plotted in Fig. 4. The Stokes $V$ profiles are reasonably well fit, but the synthetic Stokes $U$ profiles are too strongly shifted towards the red. The atmospheric parameters obtained from the fit (last line in Tab. I) turn out to be a mixture of the parameters determined from the 3-component model. The field strength, filling factor and the field azimuth ($\chi$) are similar to those of component number 1, while field inclination ($\gamma$) and temperature are more like those of component number 2. Note that the sum of the filling factors deduced with the 3-component model is approximately twice the filling factor obtained with the 2-component model (see Tab. I). This is probably due to the fact that since the two magnetic components have opposite polarities, their Stokes $V$ contributions partially cancel out, reducing the effective observed Stokes $V$ amplitude. Consequently, a large filling factor is required to reproduce the amplitudes of the observed profiles.

We were unable to obtain a reasonably accurate fit to these Stokes profiles within the confines of a 2-component model. Note, however, that since the Stokes profiles have not been observed *strictly* simultaneously we cannot

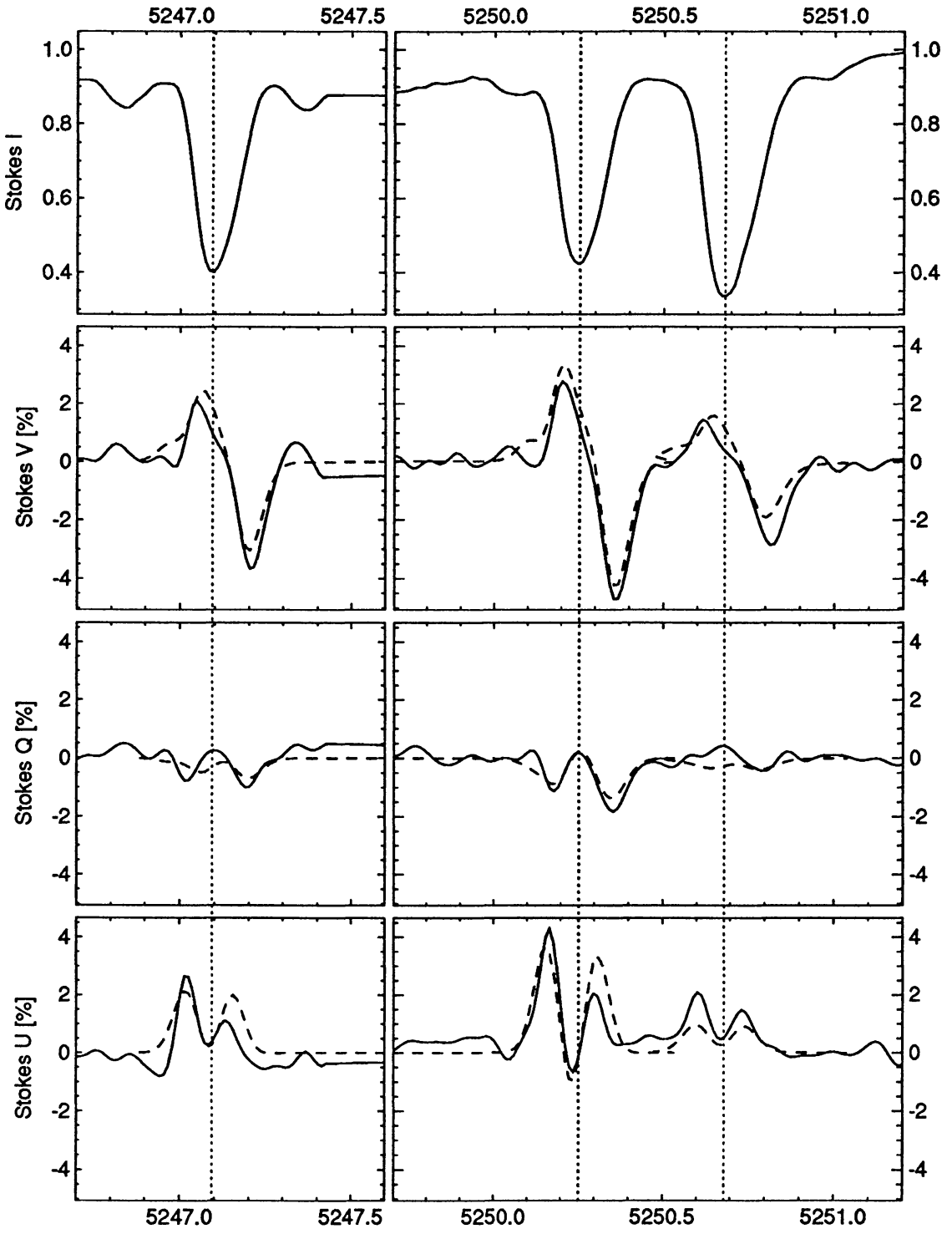


Fig. 3. Same as Fig. 1, but for another slit position. The fit parameters are: $B_1 = 1300$ G, $\gamma_1 = 117°$, $B_2 = 1580$ G, $\gamma_2 = 43°$ and $\Delta\lambda_{5250.2} = 3.5$ km/s. Note the difference between the zero crossing wavelength of the $V$ profiles (of all the lines) and the wavelengths of the Stokes $I$ minima. See the text for details.

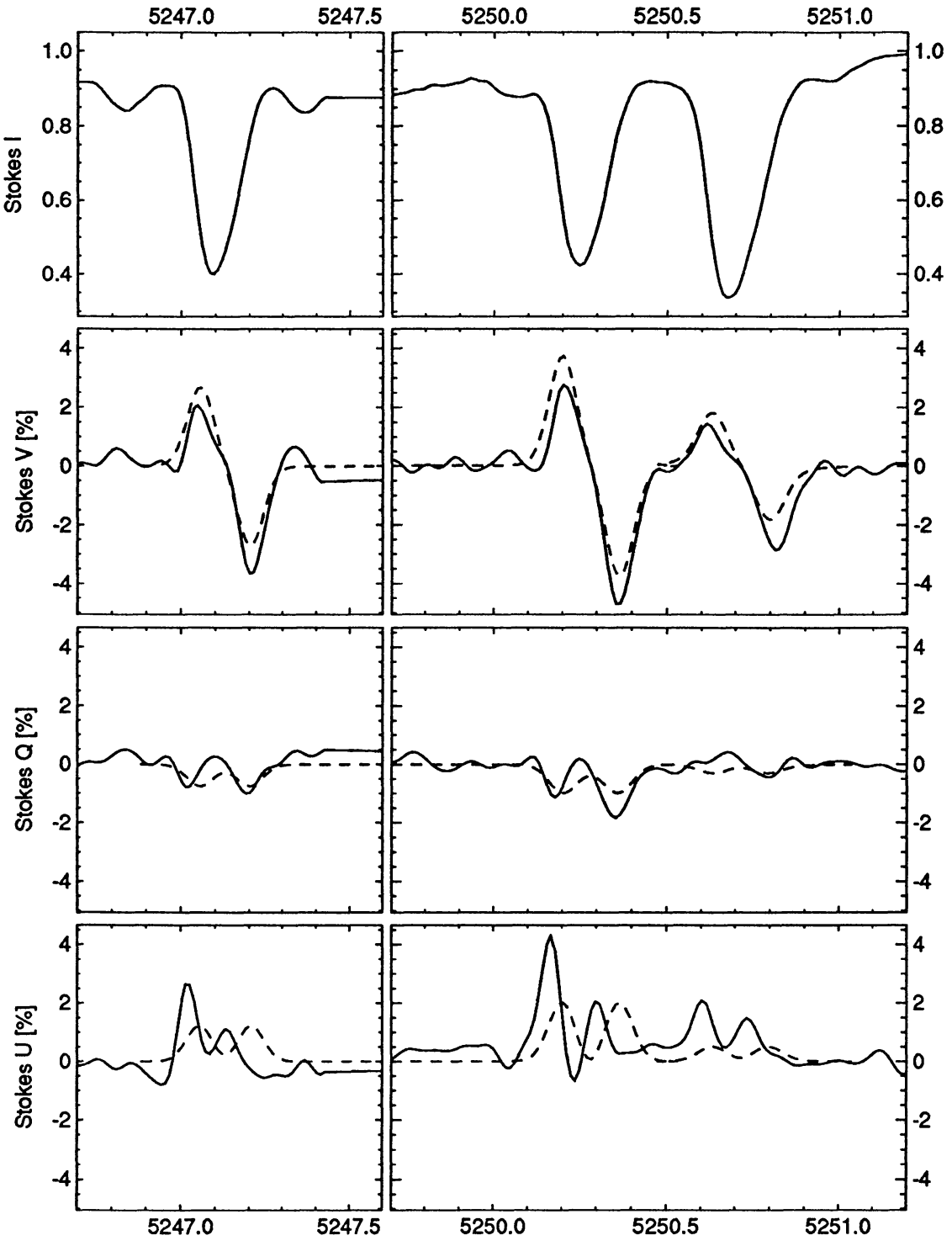


Fig. 4. Same as Fig. 3, but for a fit performed by adopting a model with just one magnetic component.

definitely rule out the possibility that the wavelength shift between $V$ and $U$ is produced by seeing effects. Nevertheless, we have demonstrated that such shifts, when present in data, can be readily explained in terms of two magnetic components. The magnitude of the shift between Stokes $V$ and Stokes $Q$ and $U$ (2 km/s) also makes it unlikely that it is an artifact.

## 5. Conclusions and final remarks

In the present work we have presented some preliminary results on the inversion of complex Stokes profiles based on a 3-component model atmosphere. Our automated approach is new for Stokes profiles produced by multiple magnetic components. In general we find that the infrared is more suited to identify the presence of multiple magnetic components than the visible, mainly due to the comparatively large Zeeman splitting in the infrared. It allows magnetic components with different field strengths to be separated easily, even if they have the same polarity and there is no velocity shift between them. In our observations the evidence for multiple magnetic components within the same resolution element is in general restricted to those cases in which the two magnetic components posses different velocity fields coupled with opposite magnetic field polarities. An exception is when the different Stokes parameters of the same spectral line exhibit different Doppler shifts, which can be explained quite naturally by a second magnetic component. In such cases the measurement of the full Stokes vector is crucial for the identification of a second magnetic component.

In general our inversion code turns out to be rather efficient in separating the two coexisting magnetic components for even relatively complex Stokes profiles. Nevertheless, for a small number of Stokes profiles it was impossible to obtain an acceptable fit even with the 3-component model. In particular $V$ profiles for which the total area under their positive part is very different from the total area of the negative part cannot be reproduced without a coupled variation of the magnetic and velocity field along the LOS. Even in the more numerous cases for which the Stokes $V$ area asymmetry is not so large we cannot rule out that part of the effect that we successfully model using two discrete magnetic components is in fact due to coupled longitudinal gradients of the magnetic and velocity fields within a single magnetic component. This basic ambiguity can probably only be successfully resolved by simultaneously considering spectral lines with widely different line strengths. (i.e. different levels of saturation).

## Acknowledgements

We are grateful to H.P. Povel and U. Egger for developing and constructing the electronics of the vector polarimeter, P. Steiner for developing the software to control it, and F. Aebersold for constructing the mechanical parts. We also thank C.U. Keller for his help during the observations and together with J.O. Stenflo for the interesting discussions on topics concerning this paper. This work was partly supported by the Swiss National Science Foundation, grant No. 20-37323.93, which is gratefully acknowledged.

## References

Bernasconi, P.N., Keller, C.U., Povel, H.P., Stenflo, J.O.: 1995, *Astron. Astrophys.* , in press

Bernasconi, P.N., Aebersold, F., Egger, U., Keller, C.U., Povel, H.P., Solanki, S.K., Steiner, P., Stenflo, J.O.: *Astron. Astrophys.*, in preparation

Emonet, T.: 1992, *Diploma Thesis*, ETH, Zürich

Keller, C.U., Bernasconi, P.N., Egger, U., Povel, H.P., Steiner, P., Stenflo, J.O.: 1995, LEST Technical Report No. 59

Maltby, P., Avrett, E.H., Carlsson, M., Kjeldseth-Moe, O., Kurucz, R.L., Loeser, R.: 1986, *Astrophys. J.* **306**, 284

Martínez Pillet, V., Lites, B.W., Skumanich, A., Degenhardt, D.: 1994, *Astrophys. J.* **425**, L113

Povel, H.P.: 1995, *Optical Engineering* **34**(7), 1870

Povel, H.P., Aebersold, H., Stenflo J.O.: 1990, *Applied Optics* **29**, 1186

Povel, H.P., Keller, C.U., Yadigaroglu, I.-A.: 1994, *Applied Optics* **33**, 4254

Press, W.H., Flannery, B.P., Teukolsky, S.A., Vetterling, V.T.: 1990, *Numerical Recipes. The Art of Scientific Computing*, Cambridge University Press, Cambridge

Rüedi, I., Solanki, S.K., Rabin, D.: 1992a, *Astron. Astrophys.* **261**, L21

Rüedi, I., Solanki, S.K., Livingston, W., Stenflo, J.O.: 1992b, *Astron. Astrophys.* **263**, 323

Ruiz Cobo, B., Del Toro Iniesta, J.C.: 1992, *Astrophys. J.* **398**, 375

Sánchez Almeida, J., Lites, B.W.: 1992, *Astrophys. J.* **398**, 359

Skumanich, A., Lites, B.W., 1991, in *Solar Polarimetry*, L. November (Ed.), National Solar Observatory, Sunspot, NM, p. 307

Skumanich, A., Lites, B.W.: 1987, *Astrophys. J.* **322**, 473

Solanki, S.K.: 1987, *Ph.D. Thesis*, ETH Zürich, p. 66

Solanki, S.K., Brigljevíc: 1992, *Astron. Astrophys.* **262**, L29

Solanki, S.K., Rüedi, I., Livingston, W.: 1992a, *Astron. Astrophys.* **263**, 312

Solanki, S.K., Rüedi, I., Livingston, W.: 1992b, *Astron. Astrophys.* **263**, 339

Solanki, S.K., Montavon, C.A.P.: 1994, *Astron. Astrophys.* **283**, 221

Stenflo, J.O.: 1968, *Acta Univ. Lund* **II**, No. 2 = *Medd. Lunds Astronom. Obs.* **II**, No. 153

Stenflo, J.O.: 1991, LEST Technical Report No. 44

Stenflo, J.O.: 1994, *Solar Magnetic Fields*, Kluwer Academic Publishers, Dordrecht, p. 320